Journal of
Mechanics of
Materials and Structures

NUMERICAL EXPLORATION OF THE DANG VAN HIGH CYCLE FATIGUE CRITERION: APPLICATION TO GRADIENT EFFECTS

Felix Hofmann, Gratiela Bertolino, Andrei Constantinescu
and Mohamed Ferjani

Volume 4, Nº 2 February 2009

mathematical sciences publishers

JOURNAL OF MECHANICS OF MATERIALS AND STRUCTURES
Vol. 4, No. 2, 2009

NUMERICAL EXPLORATION OF THE DANG VAN HIGH CYCLE FATIGUE CRITERION: APPLICATION TO GRADIENT EFFECTS

FELIX HOFMANN, GRATIELA BERTOLINO, ANDREI CONSTANTINESCU AND MOHAMED FERJANI

The objective of this paper is to show that a number of key features of the Dang Van high cycle fatigue criterion can be observed using simple polycrystalline computational models.

This paper presents a series of numerical computations for an inclusion consisting of 156 grains embedded in a homogeneous matrix. The grains are modeled using a polycrystalline single slip elasto-plastic model, whilst the matrix is considered as elastic. As expected the numerical simulations confirm the theoretical prediction on which the Dang Van fatigue criterion is based, that if a large enough number of grains is considered under uniform loading, a grain with the least favourable lattice orientation will always be present. This grain will constitute the weakest link in the assembly and thus its fatigue life largely determines the fatigue life of the bulk material.

Next the question of stress-gradients in the high cycle fatigue regime is addressed. An example of stress gradients appears around notches as they create stress concentrations in structures. It is a well known problem that fatigue criteria have to be locally arranged using stress-factors or critical distances in order to give satisfactory predictions. The work presented here shows that an analysis of the problem at the grain scale explains the apparent discrepancy when using classical fatigue criteria. The discussion is based on a numerical model of single slip crystal plasticity and the Dang Van fatigue criterion.

1. Introduction

Initially fatigue criteria were purely phenomenological, relying directly on the interpretation of experimental results at the macroscopic scale. Starting with the pioneering paper of Orowan [1939] on grain plasticity, the possibility of including grains scale effects within fatigue criteria was recognised. One of the fatigue models including grain level phenomena in a macroscopic fatigue criterion is the Dang Van–Papadopulos criterion [Dang Van 1993; Papadopoulos 1994; 1995; Dang Van and Papadopoulos 1999]. It states that fatigue does not occur if all grains reach an elastic shakedown state. In order to estimate the stress-strain state at the meso scale a simple homogenisation scheme of a plastic inclusion in an elastic matrix is considered. The keypoint of the homogenisation scheme is the assumption that any macroscopic material point includes all possible grain lattice orientations. On this basis a simple set of macroscopic formulae provide an estimate of the fatigue limit.

Since the initial Orowan grain models numerous refinements have been proposed and today complex polycrystalline grain models are available [Asaro 1983; Kothari and Anand 1998], as well as the computational power required for calculations comparable to experimental observations. Recent studies

Keywords: high cycle fatigue, fatigue criterion, polycrystalline plasticity, stress gradient, notch.
Part of the work presented in this paper was carried out by Felix Hofmann during a summer internship at the LMS funded by the CNRS.

of face centered cubic (FCC) crystal plasticity and fatigue predictions are, for example, presented in [Saanouni and Abdul-Latif 1996; Bennet and McDowell 2003; Manonkul and Dunne 2004]. Based on these models low cycle fatigue crack nucleation has been studied in [Dunne et al. 2007]. One can remark that the polycrystalline models discussed in the preceding references are rather complex. However this complexity will fade by the application of a phenomenological fatigue criterion.

This work revisits the Dang Van criterion (DVC) using a simple numerical polycrystalline model, with the specific focus of interpreting the fatigue limit as a shakedown limit for each grain. As such the proposed modeling will refine the initial closed-form homogenisation scheme.

Initially the proposed model will be used to illustrate the correct functioning of the criterion when considering a group of grains in a representative material. When the applied stress is homogeneous at the level of the representative volume element, the results of the classical closed-form homogenisation scheme are obtained. However, when a stress gradient is applied, the homogenisation assumptions are no longer valid and the numerical results illustrate the stress distribution in the grains. If the fatigue criterion is interpreted as a shakedown limit for each grain, one obtains a natural explanation of the "gradient effect" observed classically in fatigue experiments [Taylor 1999; Adib and Pluvinage 2003; Naik et al. 2005].

In our particular case, we will focus, for convenience and simplicity, on a two dimensional plane strain model of an austenitic steel with FCC crystal structure. However since we will show that the underlying homogenisation assumption breaks down in the case of a steep stress gradient, the specific case considered here (a two dimensional model and FCC structure) does not limit the generality of the observations. In fact the results and conclusions can be readily extended to three dimensions, as well as other crystallographic structures.

First a short overview of the basic assumptions of the Dang Van fatigue theory based on the shakedown concept will be given. The next section outlines the models and the computations of the simulated experiments. Finally the results are presented, firstly in the case of uniform loading, illustrating the DVC and secondly demonstrating the effect of applying a stress gradient.

2. Main assumptions of the Dang Van fatigue criterion

The fatigue analysis presented next is based on the DVC as presented in [Dang Van 1993; Papadopoulos 1995; Dang Van and Papadopoulos 1999].

Let us consider a structure under cyclic mechanical loading. Its fatigue lifetime will be determined by a number of mechanical fields: elastic and plastic strains, stresses, etc. computed over each cycle. The underlying hypothesis is that, after a short initial period of a few cycles, the mechanical response of the structure is stabilized, meaning that the fields will evolve in closed loops.

Fatigue phenomena can then be characterized at three scales:

(i) the microscopic scale of dislocations, which are the underlying elements of plastic deformation, persistent slip bands, and elastoplastic strains;

(ii) the mesoscopic scale of grains, where fatigue and damage phenomena are concentrated either at the grain boundary or in the interior;

(iii) the macroscopic scale of the structure, at which loads are applied and industrial design is performed.

An inspection of the three scales during a cyclic loading would lead to different observations determined by the fatigue regime (see Figure 1):

- In the low cycle fatigue regime, physical observations at both macroscopic and mesoscopic scale show extensive plastic strains. Moreover homogenisation theory shows that strains and stresses at the two scales tend to be closer to each other with increasing plastic strain. This can be translated into saying that the higher the applied load, the more similar mesoscopic and macroscopic scales will behave.
- In the high cycle fatigue regime, two fatigue domains corresponding to finite and infinite lifetime can be considered. Physical observations at the macroscopic scale show that structures are macroscopically in an elastic shakedown state. At the mesoscopic scale of the grains, it is now commonly accepted that elastic shakedown occurs only in the case of infinite lifetime. If lifetime is finite, some grains will be oriented such that they can not reach an elastic shakedown state, but will experience a plastic shakedown or ratcheting state leading to failure after a finite number of cycles. The stress concentration due to this mesoscopic failure marks the initiation of a macroscopic crack associated with failure on the macroscopic scale.

Focusing on the case of high cycle fatigue, one can imagine a case where only one misoriented grain is subject to plastic slip. Then a simple homogenisation scheme of a plastic inclusion in an elastic matrix can be used to derive closed-form relations between mesoscopic and macroscopic fields.

Examples of possible homogenisation assumptions are [Cano et al. 2004]:

- Lin–Taylor supposes strain equality: $\boldsymbol{\varepsilon} = \boldsymbol{E}$. This is the hypothesis of the initial Dang Van or Papadopoulos fatigue criterion.
- Sachs supposes stress equality: $\boldsymbol{\sigma} = \boldsymbol{\Sigma}$
- Kröner assumes $\boldsymbol{\sigma} = \boldsymbol{\Sigma} - \mathbb{C} : (\mathbb{I} - \mathbb{P} : \mathbb{C}) : \boldsymbol{\varepsilon}^p$, where $\mathbb{C}$ and $\mathbb{P}$ are respectively the fourth rank elastic moduli and Hill tensors and $\boldsymbol{\sigma}$ and $\boldsymbol{\Sigma}$ are respectively the mesoscopic and macroscopic stresses. In

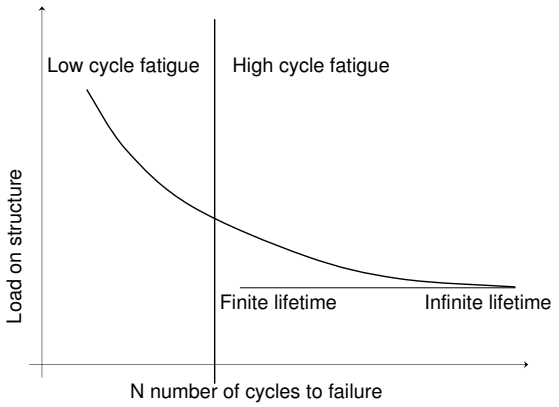

Figure 1. Illustration of high and low cycle fatigue regimes on a Whoeler diagram.

the particular case of an idealized spherical inclusion, $\mathbb{P}$ reads

$$\mathbb{P} = \frac{A}{3K}\mathbb{J} + \frac{B}{2\mu}\mathbb{K}, \qquad \text{with} \qquad A = \frac{3K}{3K+4\mu}, \qquad \text{and} \qquad B = \frac{6}{5}\frac{K+2\mu}{3K+4\mu},$$

where $\mathbb{J} = \frac{1}{3}\boldsymbol{I} \otimes \boldsymbol{I}$ and $\mathbb{K} = \mathbb{I} - \mathbb{J}$ with $\mathbb{I}$ the fourth rank identity tensor.

If, in all the cases, the same elastic behaviour at the mesoscopic and the macroscopic scale is assumed, the relation between mesoscopic and macroscopic fields can be written in the general form

$$\boldsymbol{\sigma} = \boldsymbol{\Sigma} - \mathbb{C}^* : \boldsymbol{\varepsilon}^p = \boldsymbol{\Sigma} + \boldsymbol{\rho}^*,$$

where $\boldsymbol{\rho}^*$ should be interpreted as a mesoscopic residual stress field.

The particular case of each model is obtained depending on the form of $\mathbb{C}^*$:

- for Lin–Taylor's model, $\mathbb{C}^* = \mathbb{C}$;
- for Sachs model, $\mathbb{C}^* = 0$;
- for Kröner's scheme, $\mathbb{C}^* = \mathbb{C} : (\mathbb{I} - \mathbb{P} : \mathbb{C})$.

Assuming only one active slip system generates the plastic strain

$$\boldsymbol{\varepsilon}^p = \tfrac{1}{2}\sum_s \gamma^s(\boldsymbol{m}^s \otimes \boldsymbol{n}^s + \boldsymbol{n}^s \otimes \boldsymbol{m}^s) = \sum_s \gamma^s \boldsymbol{\alpha}^s, \qquad \text{with} \qquad \boldsymbol{\alpha}^s = \tfrac{1}{2}(\boldsymbol{m}^s \otimes \boldsymbol{n}^s + \boldsymbol{n}^s \otimes \boldsymbol{m}^s).$$

The mesoscopic shear and normal stress for a slip system s with slip plane normal $\boldsymbol{n}^s$ and slip direction $\boldsymbol{m}^s$ can then be expressed as $\sigma_n^s = (\boldsymbol{\sigma} : \boldsymbol{n}^s \otimes \boldsymbol{n}^s)$ and $\tau^s = \boldsymbol{\sigma} : \boldsymbol{m}^s \otimes \boldsymbol{n}^s$.

Using the previous definitions we can define a series of fatigue criteria.

For an *individual grain*, when considering all slip systems, we have infinite lifetime if and only if

$$\max_s \max_t \big(\tau^s(t) + a\sigma_n^s(t)\big) < b,$$

where a and b are material constants and s is an index of the slip plane.

Looking at the macroscopic assembly of a number of grains g, this infinite lifetime criterion can be extended to

$$\max_g \max_s \max_t \big(\tau^s(t) + a\sigma_n^s(t)\big) < b,$$

where $\max_g$ refers to the most critical grain.

Under the assumption that the grain orientations statistically cover all directions [Papadopoulos 1994; 1995], this can be simplified to

$$\max_t \big(\tau(t) + a\sigma^H(t)\big) < b,$$

which is the classical DVC formulation. Here τ is the Tresca norm of the mesoscopic shear and $\sigma^H = 1/3\,\mathrm{tr}\,\boldsymbol{\sigma}$ is the hydrostatic stress.

We can now recall that it is currently accepted that the Papadopoulos formulation of the criterion provides practically equivalent predictions to the initial Dang Van formulation and can thus be expressed as $k^* + a\sigma_{\max}^H < b$, where k^* denotes the smallest radius of a hypersphere encompassing the stress path and $\sigma_{\max}^H$ is the maximal hydrostatic stress.

It is common to represent the stress path in a mesoscopic shear $\tau(t)$ versus mesoscopic hydrostatic stress $\sigma^H(t)$ diagram as schematically drawn in Figure 2. The line defined by the criterion is the frontier

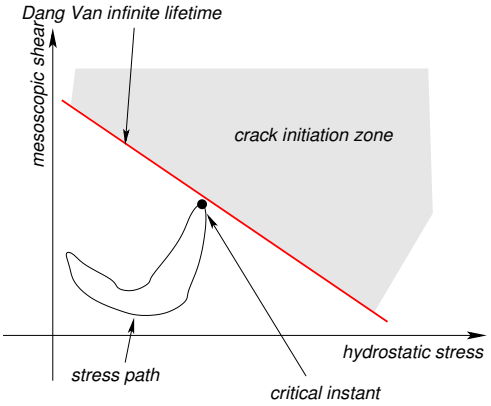

Figure 2. Illustration of the Dang Van criterion (DVC) in the τ, P plane.

between infinite life and fatigue. Component life for a load path contained completely below the DVC line will be infinite. If any point of the load path is located above the DVC line, fatigue will occur.

The parameters a and b are generally obtained from the torsion and bending fatigue limits, t_∞ and f_∞ respectively, as

$$a = \frac{t_\infty - \frac{1}{2} f_\infty}{\frac{1}{3} f_\infty}, \qquad b = t_\infty.$$

3. The experiments and their modeling

The discussion will be based on the simulation of three different setups (see Figure 3):

(i) a repeated tensile experiment (in plain strain) on a *box* specimen

$$\boldsymbol{\sigma} = \sigma_{\max} \frac{1 + \sin(t)}{2} (\boldsymbol{e}_y \otimes \boldsymbol{e}_y + \nu \boldsymbol{e}_z \otimes \boldsymbol{e}_z), \qquad t \in \mathbb{R};$$

(ii) an alternated shear experiment (in plain strain) on a *box* specimen

$$\boldsymbol{\sigma} = \tau_{\max} \sin(t) (\boldsymbol{e}_x \otimes \boldsymbol{e}_y + \boldsymbol{e}_y \otimes \boldsymbol{e}_x), \qquad t \in \mathbb{R};$$

(iii) a repeated tensile experiment (in plain strain) on a *notched* specimen

$$\boldsymbol{\sigma} = \sigma_{\max} \frac{1 + \sin(t)}{2} (\boldsymbol{e}_y \otimes \boldsymbol{e}_y + \nu \boldsymbol{e}_z \otimes \boldsymbol{e}_z), \qquad t \in \mathbb{R}.$$

Shear alternated loading was chosen instead of repeated loading, as repeated loading required an excessively large number of cycles to reach an elastic shakedown. This can be easily explained considering that onset of first mesoscopic plasticity is reached at a macroscopic shear of $\tau \approx 0.75\tau_Y$ where τ_Y is the yield limit in shear [Dang Van and Papadopoulos 1999]. Therefore the maximal macroscopic shear in repeated loading is $\tau_{\max} = 2\tau \approx 1.5\tau_Y \gg \tau_Y$.

All experiments were modeled using both a homogeneous specimen with a macroscopic homogenised constitutive law and a specimen with a polygrain inclusion embedded within a homogenised elastic

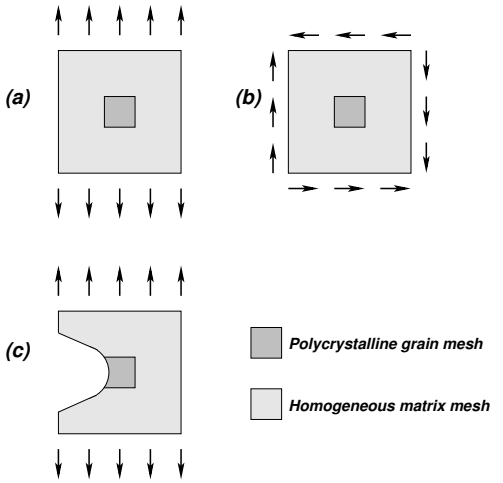

Figure 3. Illustration of the three different loading systems and the corresponding meshes which have been analysed.

material matrix (see Figure 3). The grain inclusion and the constitutive models for the grains will be described in the next section.

For simplicity the models were limited to two dimensions with plane strain condition. Loading was applied in displacement control at the mesh boundaries.

Care was taken to always remain macroscopically in the elastic shakedown state. However at the mesoscopic scale, some grains experience yielding and reach either a plastic or an elastic shakedown state after a few cycles.

Once the stabilized stress and strain fields had been obtained, the stress results of the FEM computations were post processed in the following ways:

(DV1) Computation of the DVC for each slip system in each grain (slip system projection): The DVC for each slip system is computed using the precise knowledge of the grain orientation and the slip systems of the grain. Thus one can precisely compute the mesoscopic shear and hydrostatic stress on each slip system, and compute the inequality in [Dang Van 1993] in each case in order to determine the most critical grain and slip direction.

(DV2) Computation of the Dang Van fatigue criterion in each grain: The computation of the criterion in each grain is done using the classical algorithms of the DVC with the mean stress field computed over each grain as an input value.

(DV3) Computation of the Dang Van fatigue criterion for the homogenous structure: The computation of the criterion is performed using the classical algorithms of the criterion with the stress field computed from a homogenous elastic structure submitted to the same load. In this case only the hot spot of the structure, the most critical point, is plotted in the mesoscopic shear-hydrostatic stress diagram.

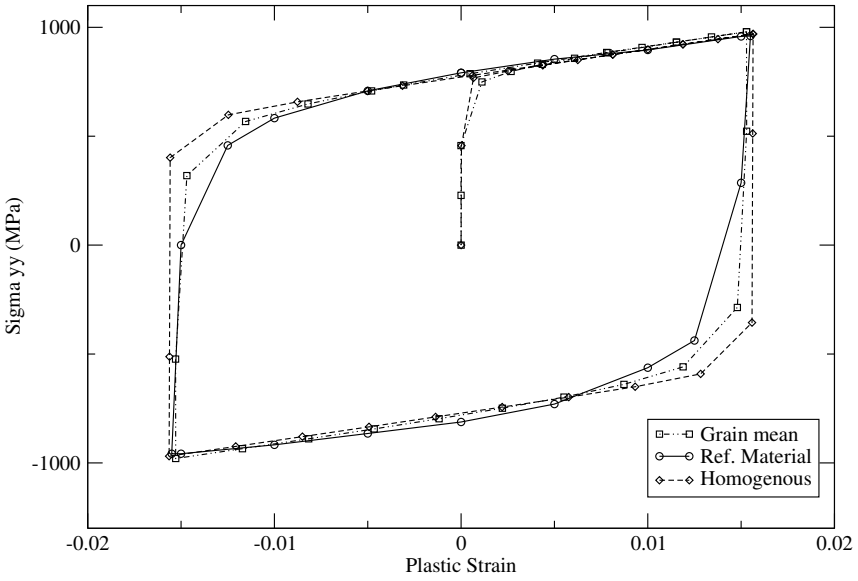

Figure 4. Macroscopic and mesoscopic material behaviour compared with experimental data averaged over a number of grains in a cyclic axial loading simulation.

4. The material

The material considered in this study corresponds to an austenitic steel with FCC crystallographic structure. The material behaviour during a cyclic tensile test is displayed in Figure 4 and has been modeled at the macroscopic scale using an elastoplastic constitutive law with linear kinematic hardening.

At the mesoscopic scale the material was modeled based on a map of grains and lattice orientations obtained from experimental observation. The grain boundaries were mapped by image processing of electronic microscopy images. Lattice orientations were found by orientation imaging microscopy using electron back scattering diffraction and were assigned in the form of Euler angles for each grain.

In this study a map of 156 grains was used (see Figure 5). Each grain was individually meshed in two dimensions using linear 3 noded elements.

The material behaviour at the mesoscopic or grain scale is captured by a simplified phenomenological elastoplastic constitutive law with linear kinematic hardening. It assumes that plastic deformation is primarily caused by crystallographic slip, which applies to most cubic crystals and some hexagonal-close-packed crystals as discussed by Weng [1983] or by Kowalczyk and Gambin [2004].

We assumed that the applied stress resolved along the slip direction on the slip plane (to give a shear stress) initiates and controls the extent of plastic deformation. Yield begins on a given slip system when the shear stress on this system reaches a critical value, the critical resolved shear stress, independent of the tensile stress or any other normal stress on the lattice plane [Bertolino et al. 2007]. For FCC lattice structure this assumption is acceptable, however in less symmetric lattices, there may be some dependence on the hydrostatic stress.

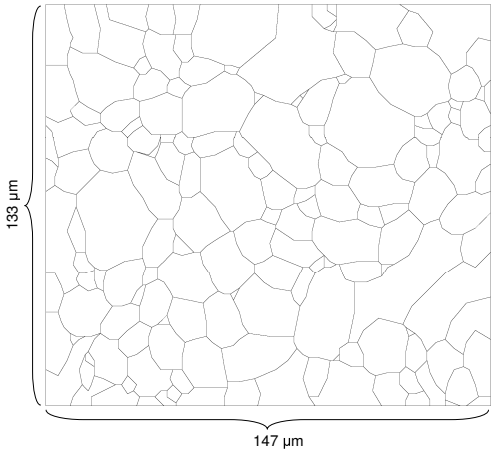

Figure 5. Grain contours of the microstructure used in this study.

For each grain g, the local yield criterion $f_g(\boldsymbol{\sigma_g})$ is obtained by the Schmid law. The individual yield stress σ_g^c depends on the active slip (gliding) system s

$$\sigma_g^c = \min_s \frac{\tau_0}{F_g^s},$$

where τ_0 denotes the critical resolved shear stress (a material parameter) and F_g^s the Schmid factor computed for each slip system using the lattice orientation provided for each grain. All twelve slip systems s of the FCC crystal structure were considered for the computation of σ_g^c and are given in Table 1. For clarity Figure 6 shows one of the FCC slip planes with its associated slip directions.

The macroscopic yield stress σ_y, the Young's modulus E, and the macroscopic kinematic hardening modulus H were identified from a macroscopic tensile test. The identification of the mesoscopic material parameters was carried out using a square grain inclusion (see Figure 5) in a square elastoplastic matrix (see Figure 3). The parameters were then adjusted to match the numerical homogenisation, that is, the averaged response over all the grains, with the macroscopic behaviour. The complete set of macroscopic material parameters is presented in Table 2.

It is important to note that, although the identification of the material parameters was carried out in the plastic regime, it was ensured that loading during the actual simulations presented next was such that the matrix always remained in the elastic regime.

Slip plane	Slip direction
(1 1 1)	[1 −1 0], [−1 0 1], [0 1 −1]
(1 −1 1)	[0 −1 −1], [1 0 −1], [1 1 0]
(−1 −1 1)	[0 −1 −1], [1 0 1], [−1 −1 0]
(−1 1 1)	[0 1 −1], [1 0 1], [−1 −1 0]

Table 1. FCC slip planes and the associated slip systems.

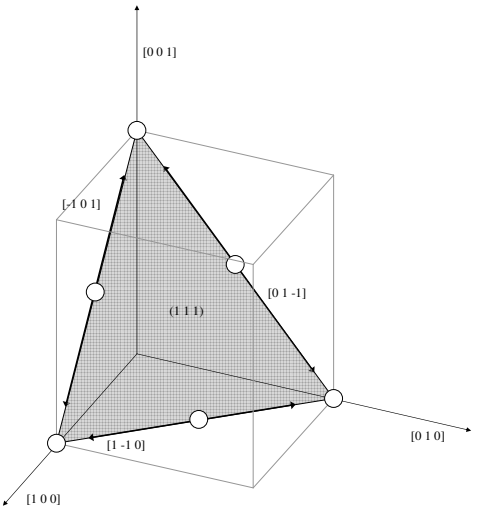

Figure 6. FCC crystal structure with one slip plane and its associated slip directions.

All finite element stress computations were performed using the object oriented finite element toolbox [Cast3M 2008] which includes a number of preprocessing, solving, and postprocessing routines. Parts of the postprocessing procedures were performed using MATLAB.

5. Results and discussion

The presentation of the numerical results is carried out by plotting the critical instant found for each grain on a Dang Van plot (see Figure 7). The critical grain instances are computed by post processing scheme 1 from the stabilised stress trajectory in each grain once a shakedown state has been reached (see Figure 2).

First, to validate the proposed approach, it was essential to verify that for tensile and shear loading, performed on the box specimen, the projection of mesoscopic shear onto crystal slip systems (post processing method DV1) leads to similar results as the DVC (post processing DV3).

To ensure that the number of grains in the grain mesh constitutes a representative sample, two further grain inclusions with randomly generated lattice orientations based on the same grain structure were generated. Figures 8 and 9 represent plots of mesoscopic shear versus hydrostatic stress of the grain critical instances for these three different distributions of lattice orientations (O_1, O_2, O_3), when subjected to macroscopic shear and tensile loading respectively.

E (GPa)	ν	σ_Y (MPa)	H (MPa)	a	b (MPa)
210.	0.3	670.	9500.	0.45	260.

Table 2. The macroscopic material parameters: E is Young's modulus, ν Poisson ratio, σ_Y the yield limit, H the kinematic hardening modulus, and a and b Dang Van fatigue parameters.

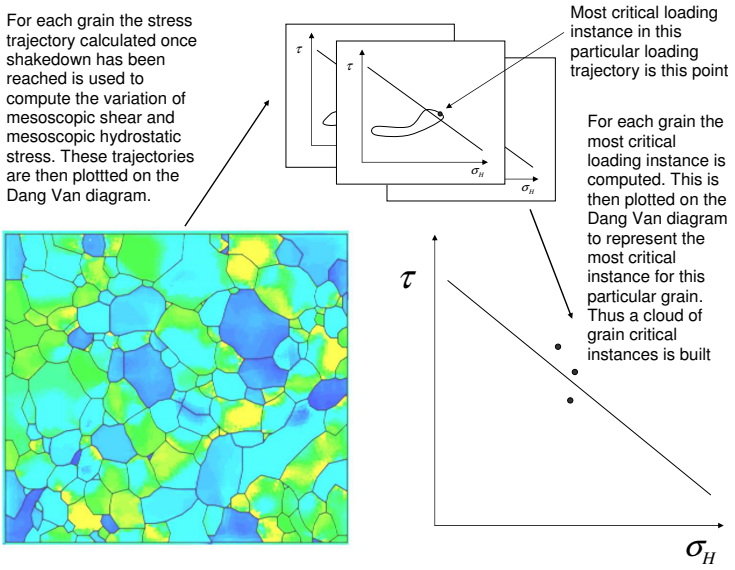

Figure 7. Plotting scheme of grain critical instances.

5.1. ***No stress gradient: box specimen.*** In each simulation, the structure was subjected to 5 cycles and the results from the last cycle were plotted. In both cases the homogeneous elastic solution has also been represented (corresponding to postprocessing DV3). One can easily remark that the clouds of grain

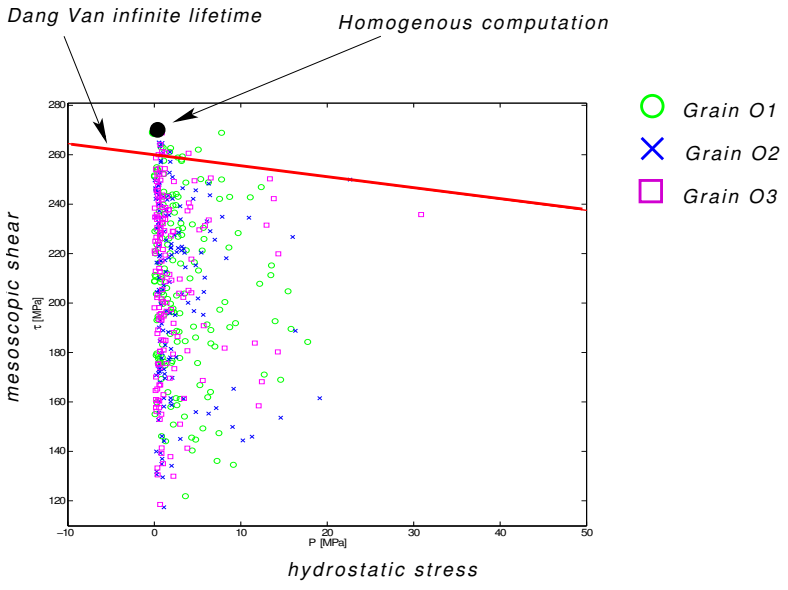

Figure 8. Three clouds of grain critical instances plotted in a Dang Van diagram of mesoscopic shear versus mesoscopic hydrostatic stress for different lattice orientations (O_1, O_2, O_3) in the case of alternated shear loading.

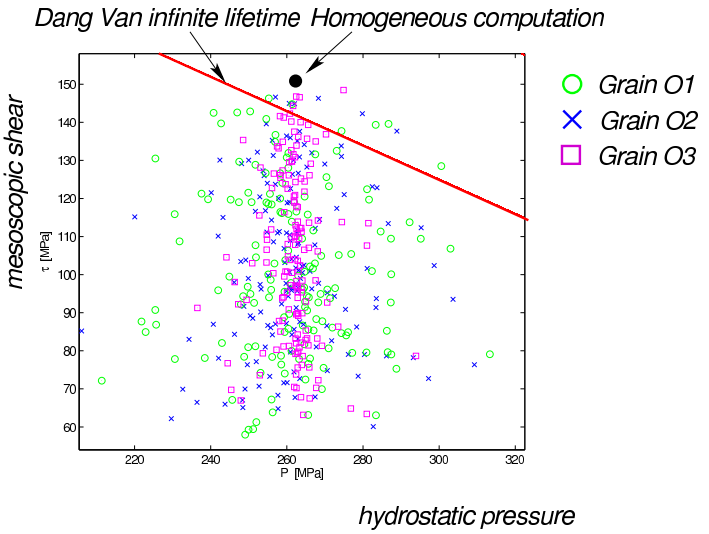

Figure 9. Three clouds of grain critical instances plotted in a Dang Van diagram for different lattice orientations (O_1, O_2, O_3) in the case of repeated tensile loading.

critical instances (see Figures 8 and 9) are just below the homogeneous critical instant and that the most critical grain approximately coincides with the homogeneous solution.

If the applied load is below the fatigue limit it can be seen that the clouds of critical instances are compact with a small range of mesoscopic hydrostatic stresses, corresponding to small pressures (see Figure 10, $\sigma_{\max} = S_2$ (shear loading) and Figure 11, $\tau_{\max} = T_2$ (tensile loading)). When loading is increased the clouds of grain critical instances closely follow the homogenous elastic solution point. Also the clouds spread out and the range of mesoscopic hydrostatic stress increases significantly (see Figure 10, $\sigma_{\max} = S_1$ (shear loading) and Figure 11, $\sigma_{\max} = T_1$ (tensile loading)). This is a direct consequence of increased grain plasticity with increasing applied load, as the hydrostatic stress range is directly related to the residual stress distribution in the individual grains. However when the residual stress average is computed across all the grains it is close to zero as one would expect. This confirms that macroscopically the homogeneous elastic solution can still be used as a reference.

The case of shear loading (see Figure 10) presents an interesting distribution of grain critical instances in the case where practically no plastic deformation has been observed. The zero mesoscopic hydrostatic stress observed in this case is coherent with and as expected for shear loading. As load increases however, the range of mesoscopic hydrostatic stresses increases and the grain critical instances spread out, as a result of the increase in grain plasticity.

5.2. ***Results and discussion: with stress gradient.*** Next we shall examine the behaviour of the grain inclusion when exposed to a stress gradient. This gradient was introduced by means of a notch with a stress concentration factor of approximately 5 (see Figure 3, configuration c)

One would expect the strain and stress distribution in the homogenous specimen to differ significantly from that in the specimen containing the granular inclusion. However, they show considerable similarity

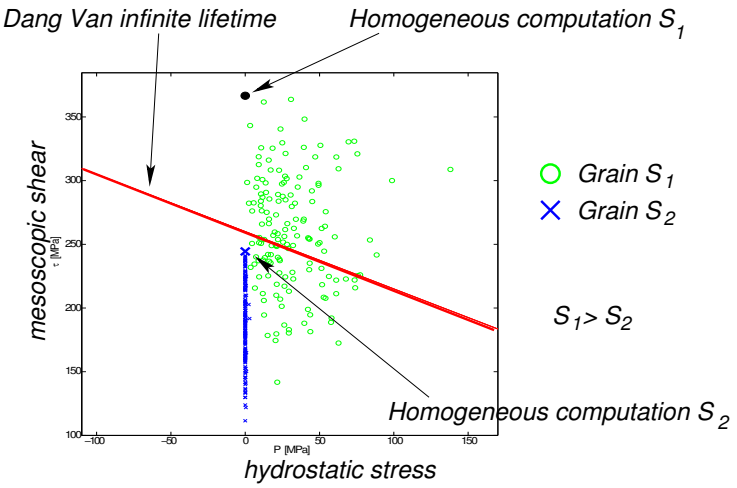

Figure 10. Two clouds of grain critical instances plotted in a Dang Van diagram for two different applied shear loads, $\tau_{\max} = S_1, S_2$.

since we primarily remain in the elastic regime which is the same for both models and only a few grains show small plastic deformations.

Figure 12 displays in a Dang Van diagram the grain critical instant clouds found in the case of repeated tensile loading of the notched specimen. For the specimen containing the granular inclusion two different clouds were computed:

- one by projecting the mesoscopic stresses onto the slip systems in each grain, and thus computing greatest mesoscopic shear and hydrostatic stress (post processing DV1), and
- one by direct application of the DVC to each grain (post processing DV2).

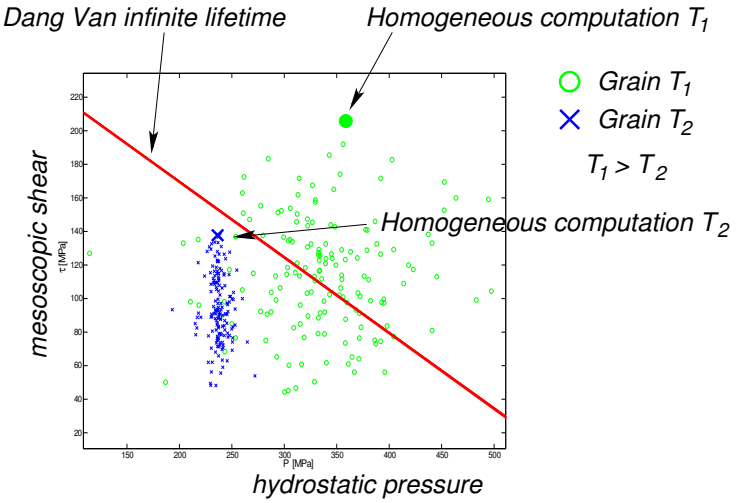

Figure 11. Two clouds of grain critical instances plotted in a Dang Van diagram for two different applied tensile loads, $\sigma_{\max} = T_1, T_2$.

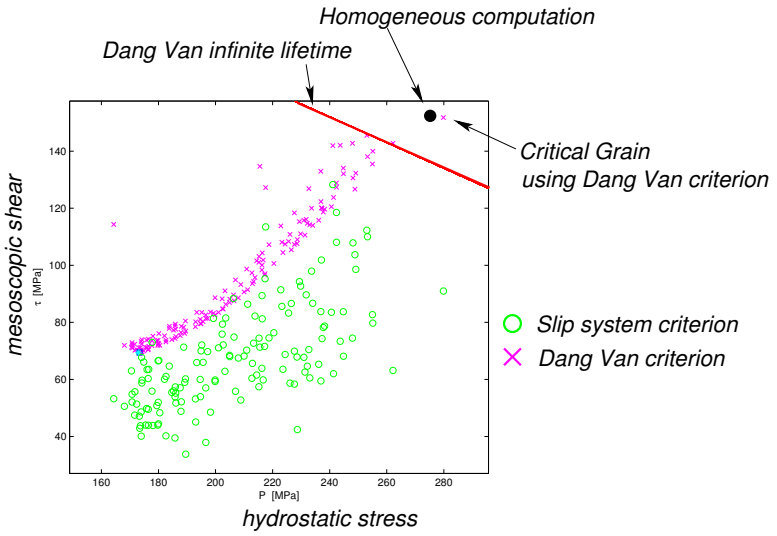

Figure 12. Two clouds of grain critical instances plotted in a Dang Van diagram for the case of repeated tensile loading for a notched specimen. The first cloud is computed by projecting the mesoscopic stresses onto the most critical slip system (post processing DV1), whilst the second cloud shows the application of the DVC to each grain (post processing DV2).

The most critical point in the cloud obtained using the grain DVC (post processing DV2) is close to the point obtained from the homogeneous solution (post processing DV3). This means that the most critical grain will experience the same damage as the notch tip, as they both experience a similar stress path.

Let us recall however that the DVC searches the mesoscopic shear on the most critical plane. In reality the likelihood that any slip system of the grain at the notch tip is aligned with the most critical plane predicted by Dang Van is small. Therefore the grain actually experiences a smaller mesoscopic shear amplitude on its active slip systems. Consequently we find that the second cloud obtained from the most critical slip system in each grain (post processing DV1) is far below the homogeneous computation point.

It is important to understand the role of the stress gradient in this setting. Because of the high stress gradient only a few grains located at the notch tip will experience the high stresses, reducing the chance of alignment of a slip system with the most critical plane. The bulk of the grains will experience a much lower stress approaching the far field stress applied to the boundaries of the notched specimen which is much lower than the stress at the notch tip.

In contrast, if the stress gradients are small, as in the box specimen, all grains experience very similar stresses and the likelihood that a slip system of a grain is aligned with the most critical plane predicted by Dang Van is high.

Figure 13 shows the distribution of grain critical instances for a notched specimen loaded in tension for a number of different randomly allocated sets of lattice orientations (O_1, O_2, O_3). As the clouds of grain critical instances occupy the same region of the Dang Van plot, the observed behaviour of the notched specimen can be seen as representative of the general case for any set of randomly distributed lattice orientations. A more quantitatively orientated investigation of the statistics of grain critical instant

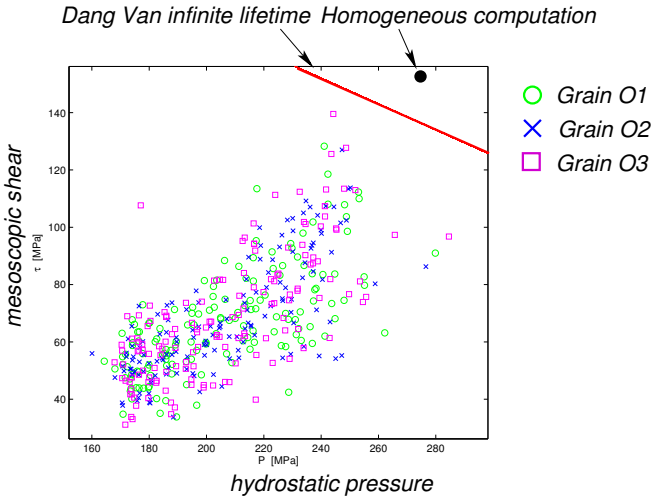

Figure 13. Three clouds of grain critical instances plotted in a Dang Van diagram for different lattice orientations (O_1, O_2, O_3) in the case of repeated tensile loading of a notched specimen.

distribution and its distance to the point of the homogeneous solution would allow the definition of an equivalent notch factor or a critical distance as usually employed in classical fatigue analysis.

When the applied load is increased (see Figure 14), the clouds of critical instances found from slip system projection in each grain (post processing DV1) follow the homogeneous solution as expected. However, we remark that the density of the cloud near the homogeneous solution is smaller than observed in the case of the box specimen. This is a direct consequence of the high stress gradient which places emphasis on a small number of grains independently of the bulk load.

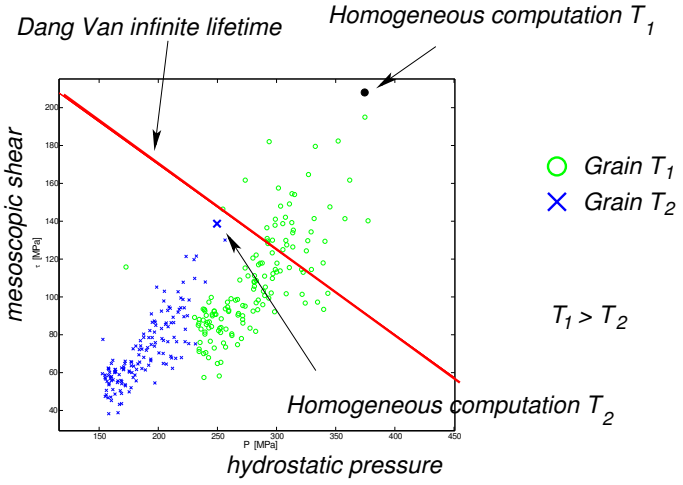

Figure 14. Two clouds of grain critical instances plotted in a Dang Van diagram for two different applied tensile loads (T_1, T_2) in the case of a notched specimen.

This observed behaviour is directly due to the breakdown of the underlying homogenisation assumption of the Dang Van fatigue criterion. In the presence of a steep stress gradient with a characteristic length scale of the same order as the local microstructural length scale, the assumption that at each material point a uniform distribution of all lattice orientations is present fails. The local number of grains at each material point is too small to constitute a macroscopic representative volume element. This breakdown of the homogenisation assumption is phenomenologically captured in the notch factor or critical distance concept in fatigue analysis.

Although the discussion here was based on a two dimensional model of an austenitic steel with FCC crystal structure, this does not limit the generality of the presented results and conclusions. The breakdown of homogenisation assumption when macroscopic loading and microstructural length scales approach can be readily extended to three dimensions and other crystal lattice structures.

6. Conclusion

In this paper a number of numerical fatigue experiments using a simplified polycrystalline model at the mesoscopic/grain scale have been presented. The impact of the applied stress gradient on fatigue life prediction was shown considering the example of a notched specimen. It was shown that high localization of stresses causes failure of the homogenisation assumptions as only few grains are exposed to very high stresses. This failure implies a fundamental change in the application of fatigue criteria in general and more particularly of critical plane criteria such as Dang Van criterion in cases of high stress gradient. The results also provide a physical explanation for critical distances and notch factors encountered in engineering practice and underline the fact that whenever the length scales of macroscopic loading and local microstructure approach, difficulties with macroscopic homogenisation assumptions will be encountered.

A finer quantitative analysis both at the meso and macroscopic levels should allow the development of a better understanding and ability to predict fatigue for stress states involving high gradients such as those found in notched or cracked specimens and bending experiments.

References

[Adib and Pluvinage 2003] H. Adib and G. Pluvinage, "Theoretical and numerical aspects of the volumetric approach for fatigue life prediction in notched components", *Int. J. Fatigue* **25**:1 (2003), 67–76.

[Asaro 1983] R. J. Asaro, "Micromechanics of crystals and polycrystals", *Adv. Appl. Mech.* **23** (1983), 1–115.

[Bennet and McDowell 2003] V. P. Bennet and D. L. McDowell, "Polycrystal orientation distribution effects on microslip in high cycle fatigue", *Int. J. Fatigue* **25**:1 (2003), 27–39.

[Bertolino et al. 2007] G. Bertolino, J. Crepin, and N. Bilger, "Modeling microstructures and microstructural effects on macroscopic and intragranular mechanical behavior", *Comput. Mater. Sci.* **40**:3 (2007), 408–416.

[Cano et al. 2004] F. Cano, A. Constantinescu, and H. Maitournam, "Critère de fatigue polycyclique pour des matériaux anisotropes: application aux monocristaux", *C. R. Mécanique* **332**:2 (2004), 115–121.

[Cast3M 2008] Cast3M, "Cast3M: an object oriented finite element toolbox", 2008, Available at http://www-cast3m.cea.fr/.

[Dang Van 1993] K. Dang Van, "Macro-micro approach in high-cycle multiaxial fatigue", pp. 120–130 in *Advances in multiaxial fatigue* (San Diego, 1991), edited by D. L. McDowell and R. Ellis, STP **191**, ASTM, Philadelphia, 1993.

[Dang Van and Papadopoulos 1999] K. Dang Van and I. V. Papadopoulos (editors), *High-cycle metal fatigue: theory to applications*, CISM Courses and Lectures **392**, Springer, Vienna, 1999.

[Dunne et al. 2007] F. P. E. Dunne, A. J. Wilkinson, and R. Allen, "Experimental and computational studies of low cycle fatigue crack nucleation in a polycrystal", *Int. J. Plast.* **23**:2 (2007), 273–295.

[Kothari and Anand 1998] M. Kothari and L. Anand, "Elasto-viscoplastic constitutive equations for polycrystalline metals: application to tantalum", *J. Mech. Phys. Solids* **46**:1 (1998), 51–67.

[Kowalczyk and Gambin 2004] K. Kowalczyk and W. Gambin, "Model of plastic anisotropy evolution with texture-dependent yield surface", *Int. J. Plast.* **20**:1 (2004), 19–54.

[Manonkul and Dunne 2004] A. Manonkul and F. P. E. Dunne, "High- and low-cycle fatigue crack initiation using polycrystal plasticity", *Proc. R. Soc. Lond. A* **460**:2047 (2004), 1881–1903.

[Naik et al. 2005] R. A. Naik, D. B. Lanning, T. Nicholas, and A. R. Kallmeyer, "A critical plane gradient approach for the prediction of notched HCF life", *Int. J. Fatigue* **27**:5 (2005), 481–492.

[Orowan 1939] E. Orowan, "Theory of the fatigue of metals", *Proc. R. Soc. Lond. A* **171**:944 (1939), 79–106.

[Papadopoulos 1994] I. V. Papadopoulos, "A new criterion of fatigue strength for out-of phase bending and torsion of hard metals", *Int. J. Fatigue* **16**:6 (1994), 377–384.

[Papadopoulos 1995] I. V. Papadopoulos, "A high cycle fatigue criterion applied in biaxial and triaxial out-of-phase stress conditions", *Fatigue Fract. Eng. Mater. Struct.* **18**:1 (1995), 79–91.

[Saanouni and Abdul-Latif 1996] K. Saanouni and A. Abdul-Latif, "Micromechanical modeling of low cycle fatigue under complex loadings, I: Theoretical formulation", *Int. J. Plast.* **12**:9 (1996), 1111–1121.

[Taylor 1999] D. Taylor, "Geometrical effects in fatigue: a unified theoretical model", *Int. J. Fatigue* **21**:5 (1999), 413–420.

[Weng 1983] G. J. Weng, "A micromechanical theory of grain-size dependence in metal plasticity", *J. Mech. Phys. Solids* **31**:3 (1983), 193–203.

Received 14 Dec 2007. Revised 14 Jun 2008. Accepted 17 Jul 2008.

FELIX HOFMANN: felix.hofmann@gmx.de
Department of Engineering Science, Oxford University, Parks Road, Oxford, OX1 3PJ, United Kingdom

GRATIELA BERTOLINO: bertolin@lms.polytechnique.fr
Centro Atomico Bariloche, 8400 San Carlos de Bariloche, Río Negro, Argentina

ANDREI CONSTANTINESCU: andrei.constantinescu@lms.polytechnique.fr
Laboratoire de Mécanique des Solides - CNRS, École Polytechnique, 91128 Palaiseau, France

MOHAMED FERJANI: ferjanimoh@yahoo.fr
Institut Français du Pétrole, 1-4 rue Bois-Préau, 92852 Rueil-Malmaison, France